

Electrochemistry of Conductive Polymers 36. pH Dependence of Polyaniline Conductivities Studied by Current-Sensing Atomic Force Microscopy

Sun-Young Hong[†] and Su-Moon Park^{*,†,‡}

School of Environmental Science and Engineering, and Department of Chemistry and Center for Integrated Molecular Systems, Pohang University of Science and Technology, Pohang 790-784, Korea

Received: January 11, 2005; In Final Form: March 15, 2005

We demonstrate from our current-sensing atomic force microscopic studies that both electrical and topographical properties of electrochemically prepared polyaniline (PAn) films are affected by their preparation conditions. The electrical properties of the fully doped PAn films prepared in 0.30 M nitric acid with its pH and ionic strength adjusted to 0.50 can be described as a conductor with an average conductivity of 49 (± 13) S/cm with primarily a compact structure resulting from a relatively small growth rate. The doped PAn films prepared at pH 5.0, for example, have compact structures with large grains and lightly doped semiconducting properties with an average conductivity of about $1.54 (\pm 0.09) \times 10^{-4}$ S/cm. From these data, we conclude that the degree of protonation of the monomers and the main reactions taking place during an early stage of the polymerization reaction are important factors determining the chemical structures as well as their conductivities and morphologies of the PAn films.

Introduction

Conducting polymers have been studied extensively during the last two decades thanks to their possible applications to a number of practical devices including sensors,¹ battery electrodes,² corrosion inhibitors,³ electromagnetic shields,⁴ and electrochromic,⁵ as well as electronic devices.⁶ Of these, polyaniline (PAn) has received more attention than most other conducting polymers because it can be straightforwardly prepared by electrochemical⁷ or chemical⁸ methods, is reasonably stable, and is reasonably conductive in their doped states.⁹ However, only PAn films prepared in strongly acidic media are known to show good electrochemical activity as well as conductivity,^{8b,10} although those prepared in neutral aqueous media have been used for incorporation of enzymes for use as sensors.¹¹ For this reason, PAn films prepared in acidic media have been characterized rather thoroughly.

The electrical properties of PAn prepared in aqueous media of different acidities have not been addressed quantitatively in the literature, although it has been pointed out by many investigators that PAn films prepared at higher pHs are not very conductive.¹² The PAns used for these measurements were prepared by chemical methods, in which aniline monomers are oxidized by ammonium persulfate in sulfuric acid. The conductivity of PAn is generally known to be strongly affected by the oxidation state as well as the degree of protonation,^{7,8b,10,12} while other conductive polymers are affected by their oxidation state alone.¹³ It is thus important to carry out a quantitative study on conductive properties of PAn films prepared in solutions of different acidities to optimize the applicability of the PAn films. The quality of films and their doping levels are much better controlled when they are prepared employing electrochemical methods.

For making nanoscopic conductivity measurements, we used atomic force microscopy (AFM) with a conducting probe in this work. The AFM with a conducting probe, also termed current-sensing AFM (CS-AFM), has found its applications in many areas during the past decade because of its ability to record topographical and current images. The technique also has a merit of establishing an easy contact with various substances including organic materials,¹⁴ which is not the case for the scanning tunneling microscopy (STM). A decided advantage of this method is that the load force can be controlled precisely for reproducible contacts between the tip and the sample. Electronic transports through single molecules,¹⁵ self-assembled monolayers,¹⁶ carbon nanotubes,¹⁷ quantum dots,¹⁸ and conducting polymer films¹⁹ have been investigated by measuring the current/voltage (I/V) traces using the CS-AFM.

In the present study, we report the effect of pH, at which the polyaniline films have been prepared, on their morphologies and electrical properties. The electrical current images obtained concurrently with the topographic images were used to calculate the conductivities of polyaniline films for more quantitative comparison.

Experimental Section

Reagent grade HNO₃ (Aldrich, 70%) and KNO₃ (Aldrich, 99.5%) were used as received, but aniline (Aldrich, 99.5%) was used after it was doubly distilled over zinc powder. Doubly distilled, deionized water was used for the preparation of solutions.

PAn films were grown on a gold-on-silicon electrode (with Cr adhesive layers, LGA films) by sweeping the potential between -0.3 and 1.1 V at a scan rate of 50 mV/s in a solution containing 50 mM aniline and an appropriate amount of HNO₃ (0.30 M) with its pH adjusted to 0.50 , 1.0 , 2.0 , 3.0 , 4.0 , or 5.0 using either 0.10 M HNO₃ or KOH, and a proper amount of KNO₃ to maintain constant ionic strengths. The total concentration of the nitrate was adjusted to 0.50 M for all solutions at

* Corresponding author. Phone: +82-54-279-2102. Fax: +82-54-279-3399. E-mail: smpark@postech.edu.

[†] School of Environmental Science and Engineering.

[‡] Department of Chemistry and Center for Integrated Molecular Systems.

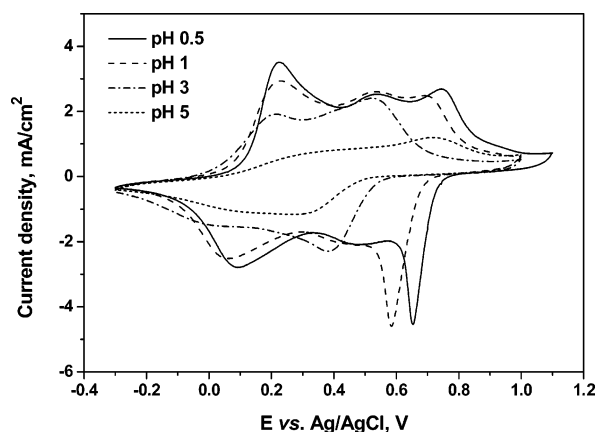


Figure 1. Cyclic voltammograms (CVs) of a PAN film recorded at different pHs of: 0.50 (—), 1.0 (---), 3.0 (- · - · -), and 5.0 (- - -), at a scan rate of 50 mV/s. The PAN film was potentiodynamically grown in a solution containing 50 mM aniline with its pH and ionic strength adjusted to 0.50.

any pH. The working electrode had an area of 0.126 cm². Before each experiment, the working electrodes were annealed for 10 min with a hydrogen flame after they were cleaned in a piranha solution (H₂SO₄:H₂O₂ = 70:30 v/v) and rinsed with deionized water. The platinum foil and Ag/AgCl (in saturated KCl) electrodes were used as counter and reference electrodes, respectively. All solutions were thoroughly deaerated by purging with a nitrogen gas (99.0%, BOC Gases) before experiments.

Electrochemical experiments were carried out with an EG&G Princeton Applied Research model 263A potentiostat/galvanostat. The contact mode AFM with a current-sensing module (PicoSPM, Molecular Imaging Inc.) was used to simultaneously obtain topographical and current images. Platinum coated cantilevers (spring constant, 0.18 N/m) were purchased from Nanosensors (<http://www.nanosensors.com>). The load force was maintained at 6–10 nN. A bias voltage between the substrate (Au) and conducting cantilever (which was grounded) was 50, 250, or 500 mV during the imaging experiments depending on how conductive the film was. PAN films prepared at each pH were doped in a nitric acid solution with its pH adjusted to 0.50 by applying an appropriate potential for 30 s, where the first oxidation peak appears, after washing thoroughly with doubly distilled water to remove oligomers or monomers. After electrochemical preparation, the films were rinsed with water again and dried by purging with the high purity N₂ gas (99.999%, BOC Gases) at room temperature and all of the AFM experiments were carried out under the controlled environment. All images were obtained across an area of 2.0 × 2.0 μm².

Results and Discussion

Figure 1a shows a series of cyclic voltammograms recorded, in a monomer-free 0.50 M nitrate solution with their pHs adjusted to 0.50, 1.0, 3.0, and 5.0 each, for a PAN film prepared in a solution containing 50 mM aniline and appropriate amounts of KNO₃ and HNO₃ to make both the ionic strength and the pH 0.50. The film thus prepared had been washed thoroughly with distilled water to remove any monomer molecules, degradation products, and excess electrolytes before cyclic voltammetric experiments were run in the above solutions. The CV recorded at pH 0.50 is in excellent agreement with those reported in the literature,⁷ showing well-defined redox peaks corresponding to a series of redox transitions: oxidation of the fully reduced, insulating form to its radical cation (polaron) at

around 0.2 V, oxidation of degradation products and/or intermediate species between 0.4 and 0.6 V, and the final transition from the delocalized polaronic state to a localized bipolaron or quinoid form above 0.7 V. The CVs recorded from the films prepared at higher pHs, however, do not display as well-defined redox reactions as that prepared at pH 0.50 (vide infra). Further, the overall charges for oxidation and reduction reactions become progressively smaller from 3.6 mC/cm² at pH 0.50 to 1.4 mC/cm² at pH 5.0, indicating that the electrochemical activity is reduced as the proton activity goes down. From just the visual inspection alone, one can see that the electrochemical activities and conductivities become deteriorated as the pH of the medium, at which the data were obtained, increases even though the film had been prepared in a medium of pH 0.50.

Figure 2 shows a series of CVs of PAN obtained during their potentiodynamic electropolymerization at pH 0.5 (a) and pH 5.0 (d), their deflection (b), as well as current (c) images of the as-prepared PAN films at pH 0.5 and pH 5.0 [(e) and (f)], respectively. A bias voltage between the substrate and the conducting cantilever was 50 mV during the imaging experiments. The typical CVs recorded during the electropolymerization of PAN at pH 0.50 shown in Figure 2a display three redox pairs as has been pointed out above during the description of the CVs in Figure 1: the first oxidation and reduction of PAN, the redox reaction of intermediate species, and the second oxidation and reduction of PAN after the first scan, which shows only an aniline oxidation peak at around 0.97 V. Figure 2d shows the electrochemical behavior during the electropolymerization of PAN at pH 5.0 under otherwise identical experimental conditions as for Figure 2a. Here, the anodic and cathodic currents corresponding to PAN redox reactions increase slowly with their peaks at about 0.6 and 0.2 V, respectively, and another current peak is observed at about 0.9 V corresponding to that of aniline oxidation, after a large anodic current is observed due to the oxidation of aniline monomers during the first scan.

To better understand the difference shown in topographic images shown in Figure 2b and e, we plotted the net anodic charges spent during the polymerization reaction as a function of the potential cycle number for the data shown in Figure 2a and d.²⁰ Figure 3 shows the net charge increases for each full potential cycle calculated by integrating the cyclic voltammetric currents shown in Figure 2a and d. The total net anodic charge consumed to deposit PAN films on the electrode surfaces was 19.73 mC (156.6 mC/cm²) at pH 0.5 and 12.44 mC (98.7 mC/cm²) at pH 5.0, respectively, during 10 potential scans. From the net anodic charge versus cycle number plot, Zotti et al. explained how a polymer grows and its morphology would be affected.²⁰ The net anodic charge, Q_{net} , which increases during the polymerization as shown in Figure 3, has the following relationship with the cycle number, CN, for the data shown in Figure 2a,

$$Q_{\text{net}} = 0.0717(\text{CN})^2 + 0.939(\text{CN}) + 2.95 \quad (1)$$

from the nonlinear curve fitting.

The growth rate expressed by eq 1 obtained for the plotted data at pH 0.50 indicates that it is primarily (~93%) linear with respect to the cycle number with a small contribution of the quadratic term (~7%), leading to the formation of an open structured polymer. The rate equation also says that the autocatalytic mechanism^{7a} accounts for a small portion of the polymer growth rate and the PAN film acts merely as a conductor. This is consistent with the results obtained in a more strongly acidic medium,²¹ where the relative contribution of the quadratic term was slightly larger than in our current experiment

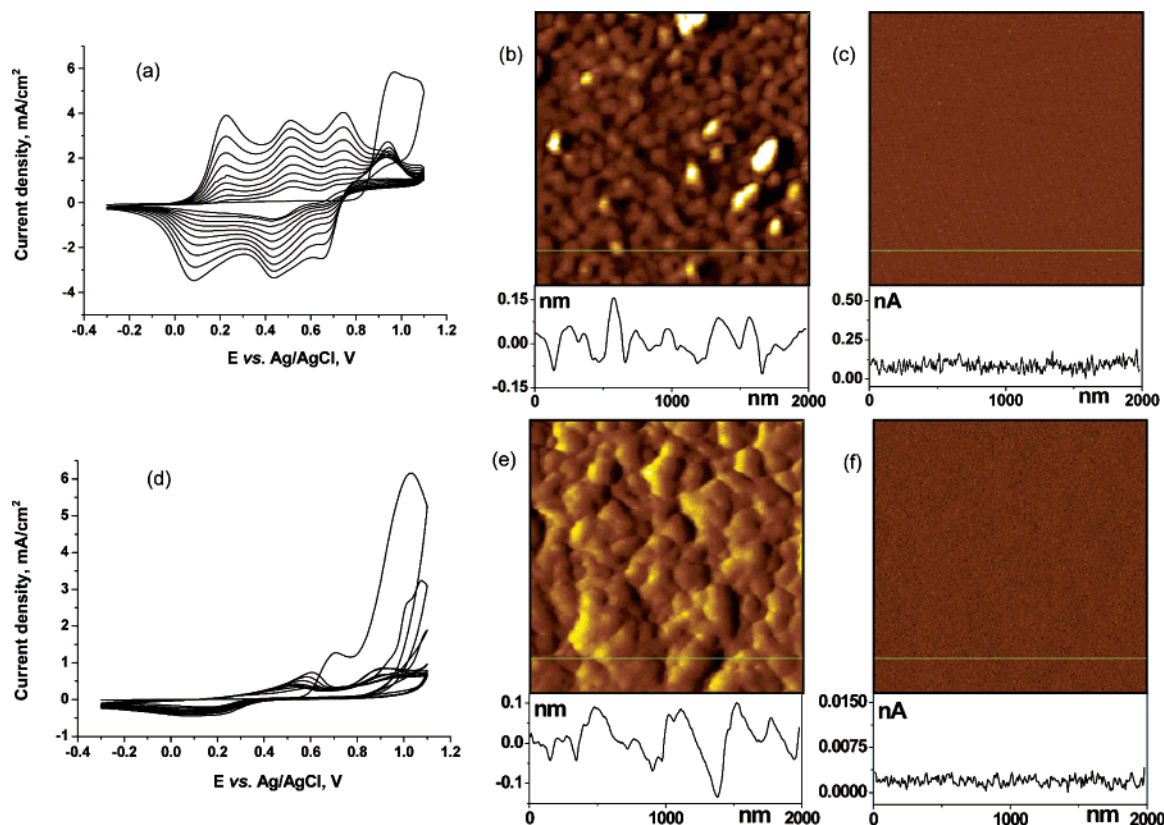


Figure 2. CVs recorded at a scan rate of 50 mV/s during potentiodynamic electropolymerization in a solution of 50 mM aniline with its pH adjusted to 0.50 (a) or 5.0 (d), their deflection as well as current image of the as-prepared PAN films at pH 0.50 [(b) and (c)], and pH 5.0 [(e) and (f)], respectively. A bias voltage between the substrate and conducting cantilever was 50 mV.

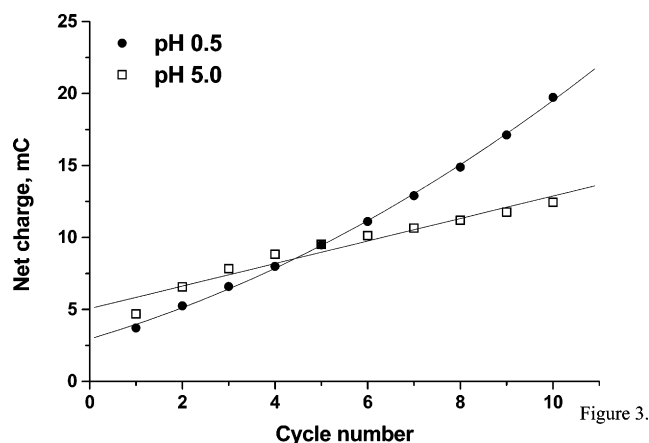


Figure 3. Net anodic charges accumulated during the potentiodynamic growth of PAN plotted as a function of the cycle number. The data were taken from Figure 2a (●) and d (□).

with its equation of $0.039(\text{CN})^2 + 0.42(\text{CN}) + 4.2$. For this reason, the deflection image of the PAN film grown at pH 0.5 (Figure 2b) shows that its morphology is less of an open structure than the one shown earlier by Choi and Park.²¹ When the growth rate is expressed by a second-order dependency, the PAN is reported to have an open structure with well-defined fibrous shapes. Another reason the morphology appears a little closer to a compact structure could be because the fibers grow vertically during the beginning of the polymer growth with the space between filled up by thickening of the fibers in later stages. The fibers were not allowed to grow long enough in 10 potential cycles as was the case in the earlier work.²¹ Most PAN fibers shown in Figure 2b appear to be the termini of the fibers growing upward.

The PAN growth rate at pH 5.0 is expressed by eq 2 in the earlier phase of growth,

$$Q_{\text{net}} = 0.782(\text{CN}) + 5.06 \quad (2)$$

which slows down even further in the later stage with no contributions from a quadratic term. Also, the coefficient of the first-order term decreases as the CN increases. The first-order dependency predicts the formation of a compact structure of the film.²⁰ The decrease in growth rate upon repeating the potential cycle is explained by the poor electrochemical activity of the PAN film formed on the electrode surface due to the difficulty in maintaining the protonated and doped structure of the polymer at pH 5.0.

As-prepared PAN films are in reduced states because the potential cycling was stopped at -0.30 V, and both the current images obtained from the films prepared at pH 0.50 and pH 5.0 shown in Figure 2c and f, respectively, exhibit relatively homogeneous current maps, in which very low currents flow between the platinum tip and the substrate. Nevertheless, the film is somewhat conductive because PAN is not completely reduced even when the potential cycle ended at -0.30 V.^{19b} Also, the average currents flowing through the film prepared at pH 0.50 is about 50 times of that prepared at pH 5.0 for the same bias voltage of 50 mV as can be seen from the current profiles shown below the current images in Figure 2c and f.

Figure 4 shows topographical (a) and current (b) images of a PAN film grown at pH 0.50 after the film was doped at 0.23 V for 30 s after degradation products and intermediate species had been completely washed off. A bias voltage between the substrate and the conducting cantilever was 50 mV during the imaging experiment. One can immediately notice that the

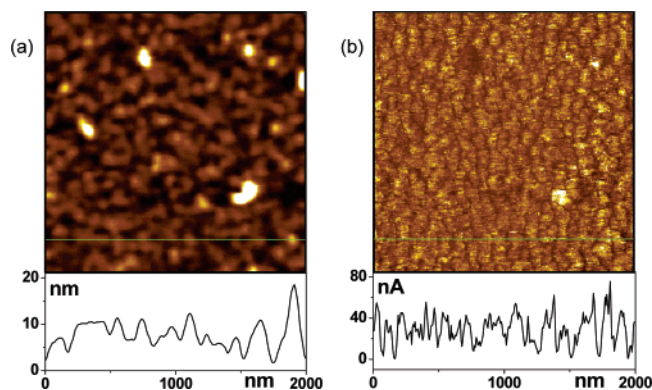


Figure 4. Topographical (a) and current (b) images simultaneously obtained for a PAN film grown at pH 0.50 after the film was doped by applying 0.23 V for 30 s after degradation products and intermediate species had been removed by thoroughly washing it.

average current obtained from the current profile of this doped PAN film is about 350 times of that for the as-prepared film shown in Figure 2c. Also, the current image matches rather well with the topographical image with low current distributions in the valleys and high currents at the center (top) of the polymer grains as can be seen from the cross-sectional profiles shown at the bottom of each image. Thus, electrical properties shown by the current image of the doped PAN film (Figure 4b) are significantly different from those by the undoped one (Figure 2c).

As described above, the conductivity of the PAN film prepared at pH 0.50 is dramatically increased when it is doped at the first oxidation peak. Han and Park^{19b} reported that the conductivity of the PAN film depends strongly on its oxidation state and also the maximum conductivity was obtained when the films were doped at 0.3 V, which is just above the first oxidation peak. The PAN films could be regarded as metallic when fully doped under these experimental conditions.

Figure 5 shows the current images recorded at a bias potential of 50 mV for the PAN films doped at pH 0.50 by applying the potential for the first oxidation of PAN for 30 s after the PAN films were grown at pH 1.0 (a), 2.0 (b), 3.0 (c), and 4.0 (d). The current images are seen to gradually change as the pH of the solution, in which the polymer was grown, is increased. The fluctuation ranges of the currents are seen from the cross-sectional profiles shown at the bottom of the images. The average current decreases steadily from 0.25 nA for the film grown at pH 1.0 to about 0.002 nA for the film at pH 4.0, as the pH, at which the polymer is grown, increases.

To compare the contact conductivities along the vertical axis of the doped and undoped PAN films prepared at pH 0.50, the slopes of the linear region of the *I/V* curves obtained for the doped (Figure 6a) and undoped films (not shown) were calculated to be 8.94×10^{-8} and 6.43×10^{-13} S, respectively. The thickness of the films was measured to be 1111 ± 280 nm from the cross-sectional view of the SEM image (not shown). The contact area between the tip and the sample was calculated to be 118.4 nm^2 from the Hertz theory.^{19b,22} From these data, the contact conductivities along the vertical axis were calculated to be $8.4 \pm 2.1 \text{ S/cm}$ for the doped film and $(6.0 \pm 1.5) \times 10^{-5} \text{ S/cm}$ for the undoped one when the PAN film was prepared at pH 0.5.

Typical *I/V* curves obtained in more conductive regions of the dried PAN films, which were prepared at pHs of (a) 0.50, (b) 1.0, (c) 2.0, (d) 3.0, (e) 4.0, and (f) 5.0 and doped at pH 0.50, are shown in Figure 6. These points were arbitrarily selected for *I/V* measurements from relatively bright spots of

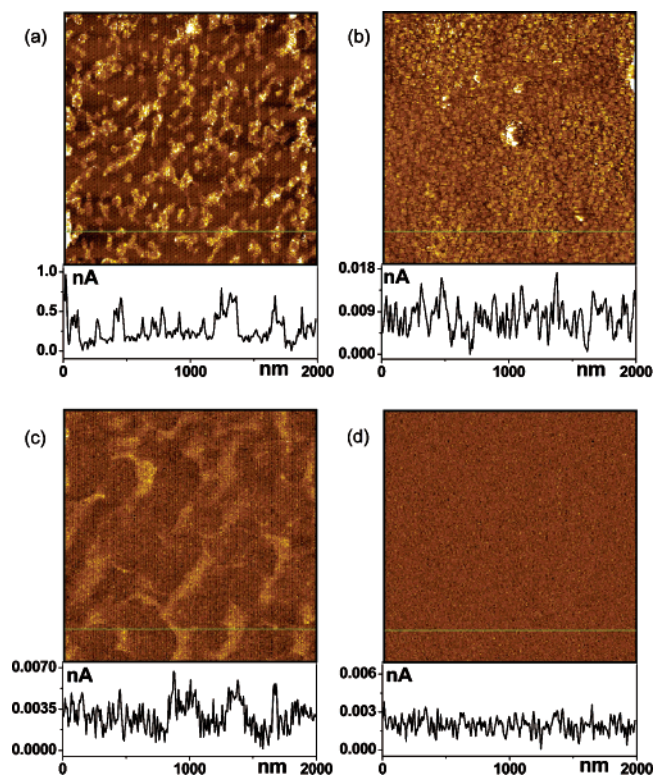


Figure 5. Current images recorded at a bias voltage of 50 mV for the PAN films doped at pH 0.50 by applying the potential (a) 0.293, (b) 0.329, (c) 0.334, and (d) 0.355 V, respectively, for 30 s after the PAN films were grown at pH: 1.0 (a), 2.0 (b), 3.0 (c), and 4.0 (d).

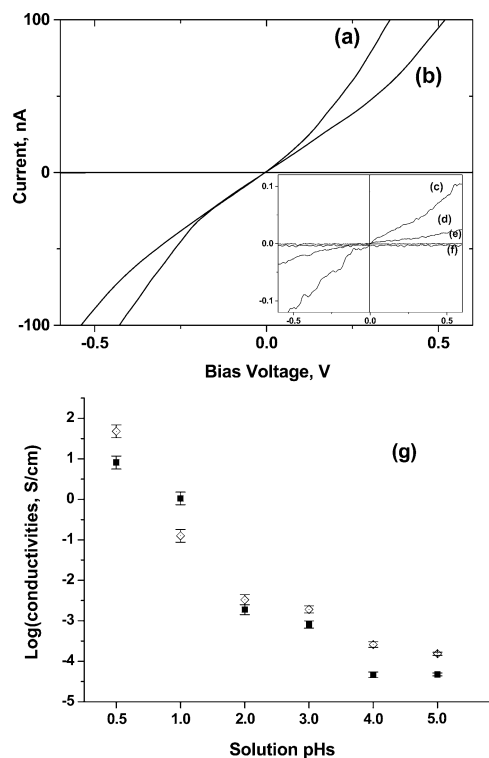


Figure 6. Current/voltage curves obtained from PAN films prepared at pH (a) 0.50, (b) 1.0, (c) 2.0, (d) 3.0, (e) 4.0, and (f) 5.0; and (g) conductivities plotted versus pH, at which the films had been prepared: contact conductivities (■) and average conductivities (□). The films were all doped at pH 0.50.

the current images for good S/N ratios. Conductivities were calculated from the slopes of the linear regions of these *I/V* curves with their thicknesses of 1111 ± 280 , 399 ± 99 , $249 \pm$

49, 243 ± 34 , 297 ± 33 , and 486 ± 28 nm, respectively, which were measured from the respective cross-sectional SEM images (not shown). Conductivities calculated from these data were 8.4 ± 2.1 , 1.1 ± 0.3 , $(1.0 \pm 0.4) \times 10^{-3}$, $(8.2 \pm 1.2) \times 10^{-4}$, $(4.7 \pm 0.5) \times 10^{-5}$, and $(4.8 \pm 0.3) \times 10^{-5}$ S/cm for PAN films prepared at pH 0.50, 1.0, 2.0, 3.0, 4.0, and 5.0, respectively. Average conductivities were calculated from at least five current profiles per a current image shown in Figures 4b, 5, and 7b by averaging currents at 256 points used for drawing the current profiles, which were taken every 7.8 nm. Average conductivities were $(4.9 \pm 1.3) \times 10^1$, $(1.3 \pm 0.3) \times 10^{-1}$, $(3.4 \pm 0.7) \times 10^{-3}$, $(1.9 \pm 0.3) \times 10^{-3}$, $(2.6 \pm 0.3) \times 10^{-4}$, and $(1.54 \pm 0.09) \times 10^{-4}$ S/cm for PAN films prepared at pH 0.5, 1.0, 2.0, 3.0, 4.0, and 5.0, respectively.

As the pH, at which PAN films were grown potentiodynamically, increases from 0.50 to 5.0, these conductivity values change from a conductor to a lightly doped semiconducting state. Figure 6g shows how the conductivities of PAN films vary as a function of pH at which they have been prepared. As can be seen from the plot, the conductivities drop nearly exponentially as the pH increases, indicating that the degree of protonation during polymerization and doping processes is very important in determining the conductivity. This is also shown by the CVs obtained during the potentiodynamic growth of PAN at pH 5.0 (Figure 2d) that low conductivities of PAN films grown at pHs higher than 2.0 result from poor electrochemical activities of the films prepared, poor protonation of the PAN films in various oxidation states, and the lack of generation of cationic (polaronic) state upon oxidation. This could be related to a detailed study of the spectroelectrochemical properties²³ as a function of the pH at which PAN films are prepared. The lack or weaker intensities of the bands corresponding to the absorption of polarons and bipolarons in the spectra recorded from PAN films prepared at higher pHs^{23a} in comparison to those recorded at pHs lower than 0.50^{23b,c} indicate that these species are not generated in the PAN films prepared at high pHs or they are not stable even if generated.

Figure 7 shows topographical (a) and current images obtained from a PAN film prepared at pH 5.0 but doped at pH 0.50 for 30 s after the potentiodynamical growth of PAN with increasing bias voltages of 50 mV (b), 250 mV (c), and 500 mV (d) at an identical full-scale current. As the bias voltages increase, magnitudes of currents measured during the imaging experiments increase as can be seen from the cross-sectional profiles shown at the bottom of the images (Figure 7b–d). It is seen that the average currents increase correspondingly as the bias voltage increases from 50 to 500 mV. The current images shown here for the doped PAN film are very similar to that recorded for an undoped PAN film prepared at pH 5.0 (Figure 2f). This shows that the electrochemically inactive nature of the films prepared at higher pHs does not lead to effectively doped states. The conductivity of the films grown at pH 5.0 is calculated to be $(2.8 \pm 0.2) \times 10^{-6}$ S/cm for the undoped PAN, whereas it is $(4.8 \pm 0.3) \times 10^{-5}$ S/cm when doped. Thus, the effect of doping is relatively insignificant in increasing the conductivities of PAN films grown at pHs higher than 2.0.

As seen above, the PAN film prepared at pH 5.0 acts as a lightly doped semiconductor even though it is fully doped by electrochemical oxidation beyond its first oxidation peak until no further anodic currents flow. We believe this is not a simple loss of its conductivity as the solution pH increases but due rather to the change in chemistry at higher pHs. Initial intermediate species produced during aniline oxidation have been known to be head-to-tail, head-to-head, and tail-to-tail type

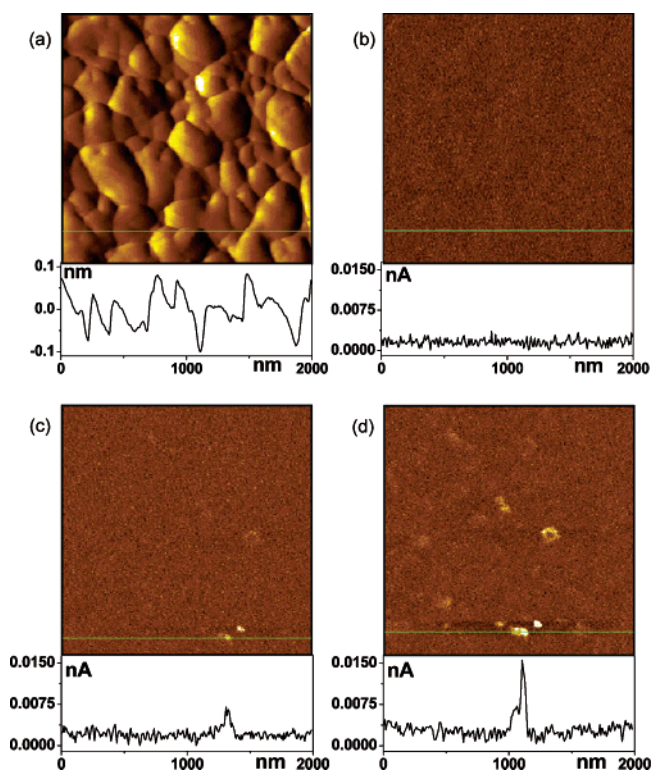


Figure 7. Topographic (a) and current images of a PAN film, which had been grown at pH 5.0 and doped at 0.394 V for 30 s at pH 0.50, recorded at different bias voltages between the substrate and conducting cantilever, 50 mV (b), 250 mV (c), and 500 mV (d).

linkages whose molar ratio depends on pH of the medium.²⁴ The different ratios of these linkages lead to different degrees of the linearity of conjugated chains and the planarity of benzene rings of the resulting polymer, which would lead to doped states of different conductivities. Ohsaka et al.²⁵ reported conductivities of PAN prepared in acidic and neutral aqueous media, as well as in nonaqueous media, using a four-point probe technique and found evidence that the structure of the PAN films changes depending on their preparation conditions. They found from their analysis of the IR spectra that the 1,4-substituted form of phenyl rings was primarily found for PAN prepared in acidic media, whereas the 1,3-substituted form was for PAN in neutral aqueous and nonaqueous media. Thus, the poor conductivities of the PAN films prepared at higher pHs are attributed to a large fraction of both head-to-head and tail-to-tail linkages introduced at an initial stage of the polymerization reaction, which limit further chain lengthening, and 1,3-linkages, resulting in cross linking. The latter would introduce the increased cross-linked fragments such as phenazine rings and/or 1,3-substituted rings in the PAN matrix rather than the linear chain grown at lower pHs. These cross-linked, as well as shorter, polymer chains lower not only the electroactivity but also conductivities of the resulting films. This explains both the poor conductivity and the slow growth shown in Figure 3 at higher pH values.

This also explains the morphologies of the PAN films grown at pH 5.0 (Figures 2e and 7a), which show large stacked grains without pores. If the PAN chain grows linearly, they would prefer to grow vertically, leading to what is called an open structure. However, the 1,3-substituted phenyl rings would result in entangled chains due to the cross-linking. Thus, the degree of protonation of the monomers or the early stage of polymerized product plays an important role in determining the chemical structure of the PAN films as well as their conductivities and morphologies.

Conclusions

We have demonstrated that the electrical and topographical properties of PAN obtained by the CS-AFM studies are affected by the preparation conditions, particularly the acidities. The electrical properties of doped PAN films prepared under acidic conditions with its pH adjusted to 0.50 can be described as a conductor with a high average conductivity of $(4.9 \pm 1.3) \times 10^1$ S/cm with compact structures resulting in a relatively small growth rate. The PAN films prepared at higher pHs having a compact structure with large grains show lightly doped semiconducting properties, and the average conductivity of the doped PAN films prepared at pH 5.0 is found to be $(1.54 \pm 0.09) \times 10^{-4}$ S/cm. From these studies, the degree of protonation of the monomers and the main chemistry taking place during an early stage polymerization are important factors affecting the chemical structure of the PAN as well as their conductivities and morphologies.

Acknowledgment. This work was supported by the grant from the KOSEF through the Center for Integrated Molecular Systems. Thanks are also due to the Korea Research Foundation for providing graduate stipends through its BK21 program.

References and Notes

- (1) (a) Service, R. F. *Science* **2001**, 293, 782. (b) Adhikari, B.; Majumdar, S. *Prog. Polym. Sci.* **2004**, 29, 699. (c) Rauen, K. L.; Smith, D. A.; Heineman, W. R.; Johnson, J.; Seguin, R.; Stoughton, P. *Sens. Actuators, B* **1993**, 17, 61.
- (2) (a) Arbizzani, C.; Mastragostino, M.; Scrosati, B. In *Handbook of Organic Conductive Molecules and Polymers*; Nalwa, H. S., Ed.; John Wiley & Sons Ltd.: Chichester, England, 1997; Vol. 4. (b) Osaka, T.; Naoi, K.; Ogano, S. *J. Electrochem. Soc.* **1988**, 135, 1071. (c) Nishio, K.; Fujimoto, M.; Yoshinaga, N.; Furukawa, N.; Ando, O.; Ono, H.; Suzuki, T. *J. Power Sources* **1991**, 34, 153.
- (3) (a) Deberry, D. W. *J. Electrochem. Soc.* **1985**, 132, 1022. (b) Wessling, B. *Adv. Mater.* **1994**, 6, 226. (c) Gašparac, R.; Martin, R. C. *J. Electrochem. Soc.* **2001**, 148, B138. (d) Kraljić, M.; Mandić, Z.; Duić, L. *Corros. Sci.* **2003**, 45, 181.
- (4) (a) Aviram, A. *Chem. Phys. Lett.* **1974**, 29, 277. (b) Park, J.; Pasupathy, A. N.; Goldsmith, J. I.; Chang, C.; Yaish, Y.; Petta, J. R.; Rinkoski, M.; Sethna, J. P.; Abruña, H. D.; Mceuen, P. L.; Ralph, D. C. *Nature* **2002**, 417, 722. (c) Park, H.; Park, J.; Lim, A. K. L.; Anderson, E. H.; Alivisatos, A. P.; Mceuen, P. L. *Nature* **2000**, 407, 57. (d) Liang, W.; Shores, M. P.; Bockrath, M.; Long, J. R.; Park, H. *Nature* **2002**, 417, 725.
- (5) (a) Lee, J.-O.; Lientschnig, G.; Wiertz, F.; Struijk, M.; Janssen, R. A. J.; Egberink, R.; Reinhoudt, D. N.; Hadley, P.; Dekker, C. *Nano Lett.* **2003**, 3, 113. (b) Kagan, C. R.; Afzali, A.; Martel, R.; Gignac, L. M.; Solomon, P. M.; Schrott, A. G.; Ek, B. *Nano Lett.* **2003**, 3, 119.
- (6) (a) Singh, R.; Lodha, A. *IEEE Trans. Semiconduct. Mater.* **2001**, 14, 281. (b) Samuel, I. D. W. *Philos. Trans. R. Soc. London, Ser. A* **2000**, 358, 193. (c) Cahen, D.; Hodes, G. *Adv. Mater.* **2002**, 14, 789. (d) He, H.; Zhu, J.; Tao, N. J.; Nagahara, L. A.; Amlani, I.; Tsui, R. *J. Am. Chem. Soc.* **2001**, 123, 7730. (e) Tour, J. M. *Acc. Chem. Res.* **2000**, 33, 791. (f) Carroll, R. L.; Gorman, C. B. *Angew. Chem., Int. Ed.* **2002**, 41, 4379.
- (7) (a) Stilwell, D. E.; Park, S.-M. *J. Electrochem. Soc.* **1988**, 135, 2254. (b) Zotti, G.; Cattarin, S. *J. Electroanal. Chem.* **1988**, 239, 387. (c) Stilwell, D. E.; Park, S.-M. *J. Electrochem. Soc.* **1988**, 135, 2491. (d) Stilwell, D. E.; Park, S.-M. *J. Electrochem. Soc.* **1988**, 135, 2497.
- (8) (a) Green, A. G.; Woodward, A. E. *J. Chem. Soc. (Trans)* **1910**, 97, 2388. (b) Huang, W.-S.; Humphrey, B. D.; MacDiarmid, J. *J. Chem. Soc., Faraday Trans. 1* **1986**, 82, 2385.
- (9) (a) Trivedi, D. C. In *Handbook of Organic Conductive Molecules and Polymers*; Nalwa, H. S., Ed.; John Wiley & Sons Ltd.: Chichester, England, 1997; Vol. 2. (b) Park, S.-M. In *Handbook of Organic Conductive Molecules and Polymers*; Nalwa, H. S., Ed.; John Wiley & Sons Ltd.: Chichester, England, 1997; Vol. 3. (c) Hugot-Le-Goff, A. In *Handbook of Organic Conductive Molecules and Polymers*; Nalwa, H. S., Ed.; John Wiley & Sons Ltd.: Chichester, England, 1997; Vol. 3.
- (10) Diaz, A. F.; Logan, J. A. *J. Electroanal. Chem.* **1980**, 111, 111.
- (11) Mu, S. L.; Xue, H. G.; Qian, B. D. *J. Electroanal. Chem.* **1991**, 304, 7.
- (12) (a) Chiang, J.-C.; Macdiarmid, A. G. *Synth. Met.* **1986**, 13, 193. (b) Genies, E. M.; Vieil, E. *Synth. Met.* **1987**, 20, 97. (c) Pingsheng, H.; Xiaohua, Q.; Chune, L. *Synth. Met.* **1993**, 57, 5008.
- (13) See chapters on conductive polymers other than polyaniline in, for example: *Handbook of Organic Conductive Molecules and Polymers*; Nalwa, H. S., Ed.; John Wiley & Sons Ltd.: Chichester, England, 1997; Vol. 2.
- (14) (a) Kelley, T. W.; Granstrom, E. L.; Frisbie, C. D. *Adv. Mater.* **1999**, 11, 261. (b) Gardner, C. E.; Macpherson, J. V. *Anal. Chem.* **2002**, 74, 576A.
- (15) (a) Cui, X. D.; Primak, A.; Zarate, X.; Tomfohr, J.; Sankey, O. F.; Moore, A. L.; Moore, T. A.; Gust, D.; Harris, G.; Lindsay, S. M. *Science* **2001**, 294, 571. (b) Cui, X. D.; Primak, A.; Zarate, X.; Tomfohr, J.; Sankey, O. F.; Moore, A. L.; Moore, T. A.; Gust, D.; Nagahara, L. A.; Lindsay, S. M. *J. Phys. Chem. B* **2002**, 106, 8609. (c) Rawlett, A. M.; Hopson, T. J.; Nagahara, L. A.; Tsui, R. K.; Ramachandran, G. K.; Lindsay, S. M. *Appl. Phys. Lett.* **2002**, 81, 3043.
- (16) (a) Sakaguchi, H.; Hirai, A.; Iwata, F.; Sasaki, A.; Nagamura, T.; Kawata, E.; Nakabayashi, S. *Appl. Phys. Lett.* **2001**, 79, 3708. (b) Wold, D. J.; Haag, R.; Rampi, M. A.; Frisbie, C. D. *J. Phys. Chem. B* **2002**, 106, 2813. (c) Beebe, J. M.; Engelkes, V. B.; Miller, L. L.; Frisbie, C. D. *J. Am. Chem. Soc.* **2002**, 124, 11268.
- (17) (a) Dai, H.; Wong, E. W.; Lieber, C. M. *Science* **1996**, 272, 523. (b) de Pablo, P. J.; Gomez-Navarro, C.; Martinez, M. T.; Benito, A. M.; Maser, W. K.; Colchero, J.; Gomez-Herrero, J.; Baro, A. M. *Appl. Phys. Lett.* **2002**, 80, 1462. (c) Li, J.; Stevens, R.; Delzeit, L.; Tee Ng, H.; Cassell, A.; Han, J.; Meyyappan, M. *Appl. Phys. Lett.* **2002**, 81, 910.
- (18) (a) Alpersen, B.; Cohen, S.; Rubinstein, I.; Hodes, G. *Phys. Rev. B* **1995**, 52, R17017. (b) Alpersen, B.; Rubinstein, I.; Hodes, G. *Phys. Rev. B* **2001**, 63, 081303.
- (19) (a) Lee, H. J.; Park, S.-M. *J. Phys. Chem. B* **2004**, 108, 1590. (b) Han, D.-H.; Park, S.-M. *J. Phys. Chem. B* **2004**, 108, 13921. (c) Lee, H. J.; Park, S.-M. *J. Phys. Chem. B* **2004**, 108, 16365. (d) Han, D.-H.; Lee, H. J.; Park, S.-M. *Electrochim. Acta* **2005**, in press.
- (20) Zotti, G.; Cattarin, S.; Comisso, N. *J. Electroanal. Soc.* **1987**, 235, 259.
- (21) Choi, S.-J.; Park, S.-M. *J. Electrochem. Soc.* **2002**, 149, E26.
- (22) (a) Israelachvili, J. *Intermolecular and Surface Forces*; Academic Press: London, 1992. (b) Riedo, E.; Brune, H. *Appl. Phys. Lett.* **2003**, 83, 1986.
- (23) (a) Hong, S.-Y.; Park, S.-M., manuscript in preparation. (b) Hong, S.-Y.; Park, S.-M. *J. Phys. Chem. B* **2005**, 109, 3844. (c) Stilwell, D. E.; Park, S.-M. *J. Electrochem. Soc.* **1989**, 136, 427. (d) Johnson, D. E.; Park, S.-M. *J. Electrochem. Soc.* **1996**, 143, 1277.
- (24) (a) Bacon, J.; Adams, R. N. *J. Am. Chem. Soc.* **1968**, 90, 6596. (b) Shim, Y.-B.; Won, M.-S.; Park, S.-M. *J. Electrochem. Soc.* **1990**, 137, 538.
- (25) Ohsaka, T.; Ohnuki, Y.; Oyama, N.; Kamisako, K. *J. Electroanal. Chem.* **1984**, 161, 399.